Solvation Dynamics of a Probe Covalently Bound to a Protein and in an AOT Microemulsion: 4-(N-Bromoacetylamino)-Phthalimide

ARTICLE *in* THE JOURNAL OF PHYSICAL CHEMISTRY B · SEPTEMBER 2002

Impact Factor: 3.3 · DOI: 10.1021/jp021046c

4 AUTHORS:

Debabrata Mandal
University of Calcutta
53 PUBLICATIONS **1,712** CITATIONS
SEE PROFILE

Sobhan Sen
Jawaharlal Nehru University
36 PUBLICATIONS **1,004** CITATIONS
SEE PROFILE

Dr. Dipankar Sukul
National Institute of Technology, Durgapur
28 PUBLICATIONS **762** CITATIONS
SEE PROFILE

Kankan Bhattacharyya
Indian Association for the Cultivation of Scie…
231 PUBLICATIONS **7,595** CITATIONS
SEE PROFILE

Solvation Dynamics of a Probe Covalently Bound to a Protein and in an AOT Microemulsion: 4-(*N*-Bromoacetylamino)-Phthalimide

Debabrata Mandal, Sobhan Sen, Dipankar Sukul, and Kankan Bhattacharyya*

Department of Physical Chemistry, Indian Association for the Cultivation of Science, Jadavpur, Kolkata 700 032, India

Amit Kumar Mandal, Rajat Banerjee, and Siddhartha Roy*

Department of Biophysics, Bose Institute, P-1/12 CIT Scheme VIIM, Kolkata 700 054, India

Received: April 24, 2002; In Final Form: July 5, 2002

4-(*N*-bromoacetylamino)-phthalimide (**I**) is used as a new solvation probe for protein and microemulsions. The photophysics of the probe 4-(*N*-bromoacetylamino)-phthalimide (**I**) is dramatically different from that of the parent compound, 4-aminophthalimide (4-AP). The solvation dynamics of **I** in an AOT microemulsion is similar to that of 4-AP in microemulsions. Solvation dynamics in the vicinity of a protein glutaminyl-tRNA synthetase (GlnRS) is studied by covalently attaching **I** to the protein. The solvation dynamics of the protein-bound probe is described by a very fast component of 40 ps and another of 580 ps.

1. Introduction

Water molecules confined in various biological and organized assemblies control the structure, function, and dynamics of biological systems in a unique way.[1] As a result, there is vigorous current interest in unraveling the behavior of water in constrained environments. In bulk water, the dielectric relaxation time is 8 ps, whereas the solvation dynamics occurs on the subpicosecond time scale.[1] In many organized assemblies, the solvation dynamics of water is described by a major component in the subpicosecond time scale similar to that of bulk water. In addition, most organized assemblies display a minor (10−30%) component on the 100−1000-ps time scale.[1−14] The latter is slower by 2−3 orders of magnitude compared to that of bulk water. Such a dramatically slow component of solvation has been detected in proteins,[2−8] cyclodextrin,[9] DNA,[10] lipid vesicles,[11] polymer−surfactant aggregates in an aqueous solution,[12] microemulsions,[13] and micelles.[14] The dynamics of many reactions depends crucially on solvation because of the differential stabilization of the transition state and the reactant. It is evident that the dramatic slowing down of solvation dynamics in biological systems seriously affects the dynamics of polar reactions (e.g., electron/proton transfer). In this work, we have investigated solvation dynamics in the immediate vicinity of a protein using a covalently attached fluorescent probe.

In a biological system, the mobility of a fluorescent probe is often studied using steady-state and time-resolved fluorescence anisotropy measurements.[15] For a probe bound to a macromolecule, the decay of fluorescence anisotropy is complicated by the overall tumbling and collective bending and twisting motions of the macromolecules that are superimposed on the motion of the fluorescent probe.[15b−d] It should be emphasized that anisotropy studies give no information on the dynamics of the solvent molecules surrounding the fluorescent probe. Recently, many groups have applied solvation dynamics to study the motion of the solvent molecules in various organized assemblies directly.[1−14] For a fluorescent probe exhibiting solvation dynamics, the fluorescence decays are markedly wavelength-dependent.[1−14] At a short emission wavelength, one observes a multiexponential decay, and at a long wavelength, a distinct rise precedes the decay. For a solvation probe, it is not straightforward to apply Perrin's equation.[15a] The latter relates the anisotropy (r) to the viscosity (η) as $(1/r) = (1/r_0) + (\tau RT/r_0\eta V)$.[15a] Because the fluorescence lifetime (τ) of a solvation probe varies with the wavelength, the anisotropy is wavelength-dependent. Furthermore, even at a fixed wavelength, drastically different anisotropy values are obtained for different lifetimes of a multiexponential decay. Because of these complications associated with the anisotropy measurements for a solvation probe and a macromolecule, we have focused our attention only on the solvation dynamics near a protein.

The study of biological water (i.e., the water molecules in the hydration layer of a protein) is of fundamental importance to understanding the role of water in biology. Using three photon echo peak shifts, Fleming et al.[3] reported that eosin bound noncovalently to a protein (lysozyme) displays a very long component of 530 ps. Such a slow component is absent in the solvation dynamics of free eosin in aqueous solution.[3] This demonstrates that the water molecules bound to the protein (lysozyme) are highly constrained. Pal et al.[4] studied solvation dynamics in human serum albumin using a noncovalently bound probe (DCM) and observed two components of 600 ps and 10 ns. Similar nanosecond components have been reported in aqueous solutions of other proteins.[5] Zewail et al.[6] studied solvation dynamics in a protein (histone) using both noncovalently and covalently attached probes and reported ultrafast solvation dynamics very similar to that of bulk water. Several groups have used the solvation dynamics of the intrinsic probe tryptophan in a protein.[7,8] Zewail et al. reported that whereas in bulk water the solvation dynamics of tryptophan occurs on a <1.1-ps time scale, in the protein subtilisin Carlsberg (SC), the solvation dynamics of tryptophan shows an additional long component of 38 ps.[7] Interestingly, when the same protein (SC) is covalently labeled with a dansyl group such that the dansyl

* Corresponding authors. E-mail: pckb@mahendra.iacs.res.in. Fax: (91)-33-473-2805.

10.1021/jp021046c CCC: $22.00
Published on Web 09/19/2002

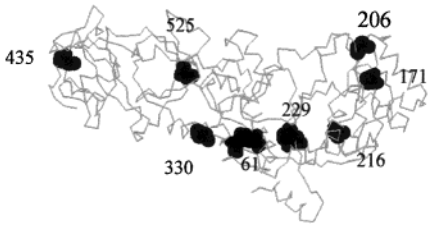

Figure 1. Crystal structure of the protein (GlnRS), showing the positions of all the sulfhydryl groups in the structure.

group resides at a distance of 7.5 Å from the protein surface, the long component (38 ps) becomes vanishingly small, and the solvation dynamics becomes almost bulk-water-like.[7] This shows that the relaxation dynamics of the water molecules near the surface of a protein depends markedly on the distance of the probe from the protein surface.

In the case of a fluorescent probe noncovalently attached to a protein, the exact location of the probe is a subject of speculation. One may get precise and unambiguous information on the solvation dynamics at selected location of a protein if and only if the probe is attached covalently to a specific site of the protein. To get such precise information, we labeled a protein covalently with a fluorescent probe. The probe is the bromoacetyl derivative of the well-known solvation probe 4-aminophthalimide (4-AP).[9c,13a,19] The probe (**I**) is obtained by the treatment of 4-AP with bromoacetyl bromide. The reaction scheme for labeling the sulfhydryl group of a protein is given in Scheme 1.

SCHEME 1: Reaction Scheme for Labeling the Sulfhydryl Group of GlnRS with 4-(*N*-Bromoacetylamino)-phthalimide (I)

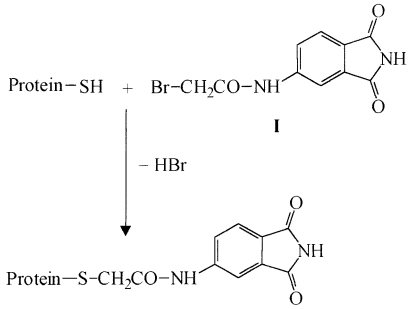

For this study, we have chosen a large protein glutaminyl-tRNA synthetase (GlnRS) isolated from *E. coli*. GlnRS is a multidomain protein of molecular mass 64 kDa. GlnRS contains eight half-cysteines and one disulfide bond.[16,17] The crystal structure of the protein[16] (Figure 1) shows positions of all the sulfhydryl groups in the structure. There are several cysteines near the surface of the protein, which are exposed to and may be accessible for labeling. Rould et al.[16] studied the reactivity of various cysteins of GlnRS toward heavy-atom (e.g., Au, Hg, etc.) reagents. Using X-ray crystallography, they showed that cysteine 206 is the most reactive sulfhydryl and the most probable site for heavy-atom labeling. It is highly exposed and resides near the surface of the protein. Under the condition of our experiment, only one probe (**I**) molecule is attached to the protein. On the basis of previous reactivity studies[16,17] we expect that the probe (**I**) is attached to the most reactive cystein 206. Thus, the probe reports dynamics at a specific site of GlnRS.

It should be noted that all the reactive sulfhydryl groups of GlnRS are located outside the active site.[17] Furthermore, we showed earlier that the biological activity of GlnRS is not altered on labeling with a fluorescent probe.[17] In our previous work,[17] we labeled GlnRS with three different probe molecules, DTNB, acrylodan, and pyrene maleimide. The sizes and natures of all three probes are different, with probe **I** closely resembling acrylodan in size and chemical nature. Pyrene maleimide is substantially larger whereas DTNB is smaller than **I**. In all cases, the biological activity and other properties of the labeled protein were found to be similar to those of native GlnRS. Thus, modification of GlnRS with probe **I** at a peripheral sulfhydryl group is very likely to preserve the native conformation and biological activity of GlnRS. Thus, the solvation dynamics reported by **I** bound to GlnRS faithfully reports the dynamics near the protein.

The purpose of this work is three-fold. First, we introduce a new solvent-sensitive fluorescent probe, 4-(N-bromoacetylamino) phthalimide (*I*). Second, we show that **I** is a sensitive solvation probe for microemulsions. Finally, we study the solvation dynamics at a specified site of protein GlnRS by covalently attaching the probe to it.

2. Experimental Section

4-AP (Kodak) was purified by repeated recrystallization from a 1:1 alcohol−water mixture. Dichloromethane was refluxed and then distilled over anhydrous P_2O_5. Triethylamine (Et_3N) was distilled over solid KOH. Bromoacetylbromide (Lancaster) was distilled before use.

The derivative (**I**) was prepared by dissolving 4-AP, bromoacetylbromide, and triethylamine in a molar ratio of 1:10:5 in dichloromethane. The reaction was quenched after 30 min using a slight excess of water. The solid product was filtered, washed several times by dichloromethane, and recrystallized from a 1:1 alcohol−water mixture.

The purity of recrystallized 4-AP and the product (**I**) was checked by ^{1}H NMR (500 MHz) using DMSO-d_6 as the solvent. 4-AP exhibits an amido proton signal at a chemical shift of 10.5 ppm and an amino proton signal at 1.8 ppm. On acetylation, the signal due to the amino group completely vanishes, and additional peaks are observed at 11 and at 3.9 ppm corresponding to the amido and methylene protons, respectively, of the $BrCH_2CONH-$ moiety.

For the preparation of the microemulsion, sodium dioctylsulfosuccinate (AOT, Aldrich) was used as received. It was dried under vacuum for 3−4 h just before use. A Karl Fischer titration shows that AOT dried in this manner contains very few water molecules. There is 1 water molecule per 10 molecules of AOT so that the water-to-surfactant (AOT) molar ratio, w_0, is 0.1 for AOT dried in vacuum. The 4-AP derivative, **I**, is nearly insoluble in *n*-heptane, but its solubility increases in the presence of 0.09 M AOT. To a solution of 0.09 M AOT in *n*-heptane, solid **I** was added, and the solid was allowed to stand for a few hours. The supernatant liquid was decanted and filtered, and to it water was added using a microliter syringe in order to get the required w_0 value. All solvents used were distilled prior to use. The procedure for the isolation and purification of GlnRS is described in our earlier work.[17]

Labeling of the protein was done as follows. To a 60 μM solution of GlnRS in 0.1 M potassium phosphate (KP) buffer (pH 7.5), a DMSO solution of the probe (**I**) was added dropwise with thorough shaking. The ultimate probe concentration in the protein solution was 200 times that of the protein, and the concentration of DMSO was less than 2 wt %. After 15 min, the reaction was quenched by adding 5 mM β-mercaptoethanol. The labeled protein solution was then dialyzed for 3 days in deaerated 0.1 M KP buffer of pH 7.5 to remove unreacted probe and other small molecules. On the basis of the extinction

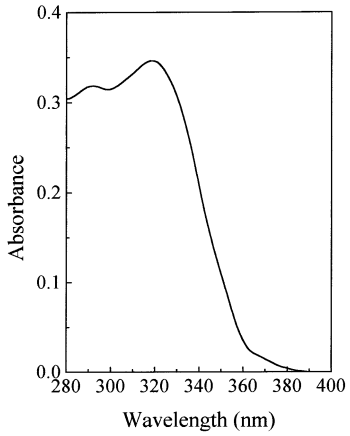

Figure 2. Absorption spectrum of 7×10^{-5} M **I** in methanol.

coefficient of the probe (**I**) and the absorbance of the solution of the protein labeled with the probe, the concentration of the bound probe is estimated to be 60 μM. Because the concentration of the protein is also 60 μM, one may assume that only one probe is attached to each protein molecule. For the probe covalently attached to GlnRS, the steady-state fluorescence anisotropy is found to be 0.13. This is much higher than the anisotropy (r) of the free probe (**I**) in aqueous solutions (r = 0.02). The high anisotropy indicates restricted mobility of the probe on attachment to GlnRS.

All NMR spectra were recorded on a Bruker DRX-500 spectrometer with a standard pulse sequence. The steady-state absorption and emission spectra were recorded on a JASCO 7850 spectrophotometer and a Perkin-Elmer 44B spectrofluorimeter, respectively. The emission quantum yield (ϕ_f) was determined using the reported ϕ_f = 0.01 value for 4-AP in water.[19d]

For lifetime measurements, the sample was excited at 300 nm by the second harmonic of a rhodamine 6G dual-jet dye laser with DODCI as the saturable absorber (Coherent 702-1) synchronously pumped by a CW mode locked Nd:YAG laser (Coherent Antares 76s). The emission was collected at magic angle polarization using a Hamamatsu MCP photomultiplier (2809U). Our time-correlated single-photon counting (TCSPC) set up consists of Ortec 935 QUAD CFD and Tennelec TC 863 TAC. The data are collected with a PCA3 card (Oxford) as a multichannel analyzer. The typical fwhm of the system response is about 50 ps.

3. Results

3.1. Emission Properties of I in Neat Solvents. Figure 2 shows the absorption spectrum of **I** in methanol. It is readily seen that the absorption spectrum of **I** is markedly blue-shifted from those reported earlier for 4-AP. For instance, in a polar solvent (water or methanol), 4-AP exhibits two peaks at around 310 and 360 nm,[19] whereas **I** shows two peaks at around 290 and 320 nm.

Figure 3 shows the emission spectra of **I** in different solvents. The emission maxima of **I** in water, methanol, acetonitrile, and dioxane are at 460, 440, 395, and 390 nm, respectively. The emission maxima of **I** in different solvents display large blue shifts from those of 4-AP in the same solvents.[19] Emission quantum yields of **I** are 0.4, 0.75, 0.2, and 0.006, respectively, in water, methanol, acetonitrile, and dioxane. Values of the lifetime of **I** are 8, 12, 2.1, and 0.22 ns in pure water, methanol, acetonitrile, and dioxane, respectively. The very high emission quantum yield and lifetime of **I** in protic solvents (water and methanol) compared to those in aprotic solvents (e.g., acetonitrile and dioxane) are in sharp contrast to the emission behavior of 4-AP. 4-AP exhibits a very low emission quantum yield (ϕ_f = 0.01) and short lifetime (1.1 ns) in water and exhibits a very high emission quantum yield (ϕ_f = 0.7) and long lifetime (15 ns) in an aprotic solvent, dioxane.[19]

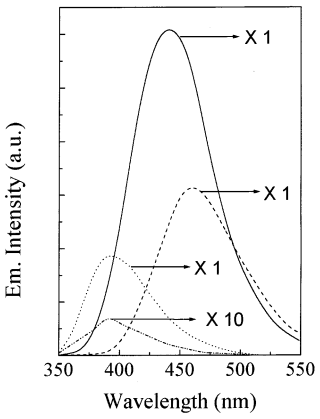

Figure 3. Emission spectra of 7×10^{-5} M **I** in water (- - -), methanol (—), acetonitrile (···), and dioxane (10 times amplified) (-···-).

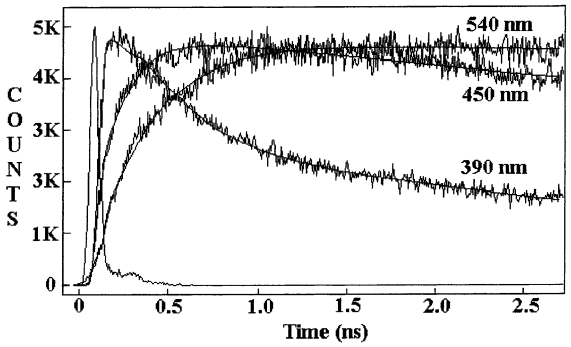

Figure 4. Fluorescence decays of 7×10^{-5} M **I** in an AOT microemulsion (w_0 = 20) at 390, 450, and 540 nm.

In aqueous solutions, the fluorescence decays of **I** show no wavelength dependence. This is quite expected because in bulk water the solvation dynamics occurs on a 1-ps time scale, which is faster than the response time of our set up (50 ps). In the following sections, we will show that in microemulsions and in the vicinity of a protein the solvation dynamics of **I** is much slower.

3.2. Emission Properties of the 4-AP Derivative (I) in AOT Microemulsions. In a reverse micelle containing 0.09 M AOT in *n*-heptane, the emission quantum yield (ϕ_f) of **I** is 0.13 with the emission maximum at 390 nm, which is blue-shifted by 70 nm from that in water (460 nm). On addition of water, the absorption spectrum of **I** in an AOT microemulsion does not change perceptibly. However, in an AOT microemulsion on addition of water, the emission intensity of **I** gradually increases with a significant red shift up to w_0 = 12. For $w_0 \geq 12$, the steady-state emission spectrum of **I** in an AOT microemulsion remains more or less unchanged. At w_0 = 12, the emission intensity of **I** increases ~4 times, and the emission maximum exhibits a red shift of 60 to 450 nm relative to that at w_0 = 0.1. The increase in the emission quantum yield of **I** in microemulsions with an increase in w_0 is in sharp contrast to the behavior of 4-AP, whose emission quantum yield decreases with increasing w_0.[13a]

Figure 4 shows fluorescence decays of **I** in an AOT microemulsion at w_0 = 12. It is readily seen that there is a marked wavelength dependence of decays. At the blue end (390

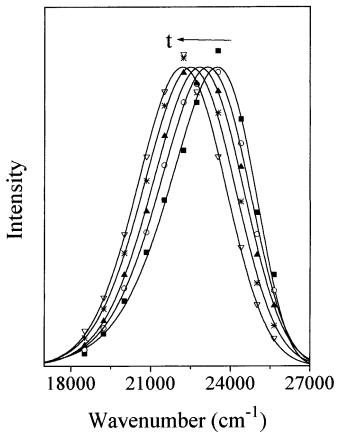

Figure 5. Time-resolved emission spectra of **I** in an AOT microemulsion ($w_0 = 20$) at 0 (■), 100 (○), 250 (▲), 700 (∗) and 20 000 ps (▽).

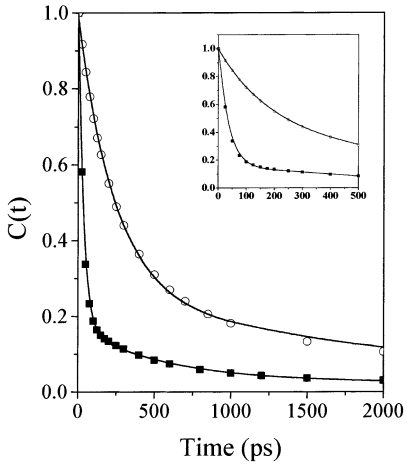

Figure 6. Decay of response function, $C(t)$, of **I** in an AOT microemulsion ($w_0 = 20$, ○) and covalently bound to GlnRS in 60 μM GlnRS in phosphate buffer (pH = 7.5, ■). The points denote the actual values of $C(t)$, and the solid line denotes the best fit to a biexponential decay. The initial part of the decays of $C(t)$ are shown in the inset.

nm) of the emission spectrum, only a long decay with the 440-ps (60%) and 10.2-ns (40%) components is observed, whereas at the red end (540 nm), the decay of 10.9 ns is preceded by a distinct rise of 400 ps. Such wavelength dependence clearly indicates that inside the AOT microemulsion of $w_0 = 12$, the 4-AP derivative (**I**) exhibits very slow solvation dynamics. From the parameters of best fit to the emission decays and using the steady-state emission spectra, time-resolved emission spectra (TRES, Figure 5) of **I** in an AOT microemulsion ($w_0 = 12$) have been constructed following the procedure described by Fleming and Maroncelli.[18] The solvation dynamics is described by the decay of the response function $C(t)$, which is defined as

$$C(t) = \frac{\nu(t) - \nu(\infty)}{\nu(0) - \nu(\infty)}$$

where $\nu(0)$, $\nu(t)$ and $\nu(\infty)$ denote the observed emission energies (frequencies) at time zero, t, and infinity. The total Stokes shift in our setup, $\Delta\nu = \nu(0) - \nu(\infty)$, of (**I**) in the water pool of an AOT microemulsion is found to be 1300 cm^{-1}. The decay of $C(t)$ for the 4-AP derivative (**I**) inside an AOT microemulsion ($w_0 = 12$) is shown in Figure 6, and the decay parameters of $C(t)$ are summarized in Table 1. The decay of $C(t)$ is found to be biexponential with one component of 230 ps (70%) and a very long component of 2100 ps (30%) with an average

TABLE 1: Decay Characteristics of 4-(*N*-Bromoacetylamino)-phthalimide

system	$\Delta\nu$ (cm^{-1})	a_1	τ_1 (ps)	a_2	τ_2 (ps)	$\langle\tau_s\rangle^a$ (ps)
AOT microemulsion	1300	0.70	230 ± 50	0.30	2100 ± 50	790
GlnRS	1330	0.85	40 ± 10	0.15	580 ± 50	120

[a] $\langle\tau_s\rangle = a_1\tau_1 + a_2\tau_2$, ±50 ps.

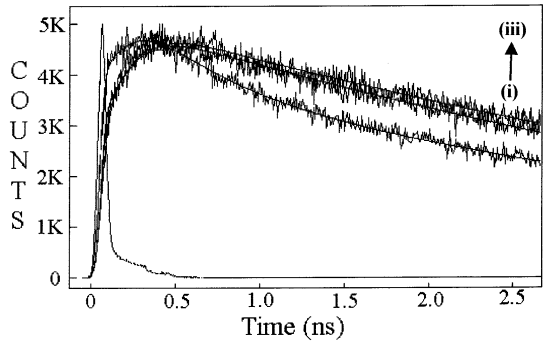

Figure 7. Fluorescence decays of **I** covalently bound to GlnRS in 60 μM GlnRS in phosphate buffer (pH = 7.5) at (i) 410, (ii) 460, and (iii) 540 nm.

solvation time of 800 ± 50 ps. It may be recalled that in microemulsions many probes, including 4-AP, are reported to have average solvation times of 1000−2000 ps.[1,13] The observed average solvation time of **I** in AOT microemulsions is close to this.

3.3. Emission Properties of I Covalently Attached to a Protein, Glutaminyl-tRNA Synthetase. In an aqueous solution containing 60 μM GlnRS in phosphate buffer (pH = 7.5), the emission maximum of the covalently bound probe is found to be at 460 nm. This indicates that the probe bound to one of the −SH groups of the protein experiences a microenvironment that is not much different from that of the bulk water. Thus, it is inferred that the probe molecule (**I**) binds to one of the −SH groups that is largely exposed to bulk water.

Whereas the steady-state emission spectrum of the probe bound to protein is similar to that of the free probe in bulk water, the time-resolved studies indicate substantial differences. As shown in Figure 7, emission decays of the probe (**I**) bound to the protein are markedly wavelength-dependent. At short wavelengths (e.g., 410 nm), we observed a fast decay with components of 370 ps (30%) and 5.6 ns (70%). However, at long wavelengths (540 nm), the decay of 6.34 ns is preceded by a distinct rise of 40 ps. Such a wavelength dependence clearly indicates that in the protein environment the water molecules around the probe exhibit slow solvation dynamics. The time-resolved emission spectra (TRES, Figure 8) of the 4-AP derivative (**I**) in GlnRS were constructed from the parameters of best fit to the emission decays and using the steady-state emission spectrum. The decay of $C(t)$ for **I** bound to GlnRS is shown in Figure 6. The decay parameters of $C(t)$ are summarized in Table 1. The total Stokes shift, $\Delta\nu = \nu(0) - \nu(\infty)$, of **I** in 60-$\mu$M GlnRS is found to be 1330 cm^{-1}. The decay of $C(t)$ of **I** in GlnRS is found to be biexponential, with one component of 40 ps (85%) and a very long component of 580 ps (15%)

4. Discussion

The most important finding of this work is obviously the direct and unambiguous study of the solvation dynamics in a well-defined location of the protein GlnRS using a covalently bound probe. But before discussing that, we will highlight the

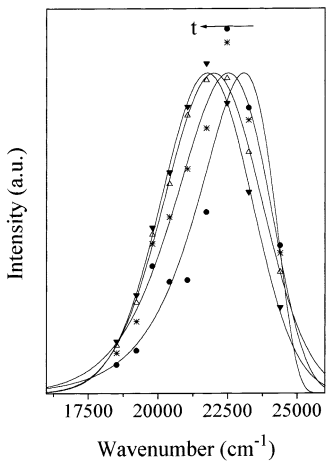

Figure 8. Time-resolved emission spectra of **I** covalently bound to GlnRS at 0 ps (●), 25 (∗), 100 (△) and 5000 ps (▲).

dramatic differences in the solvent dependence of the emission properties of **I** from those of the parent compound, 4-AP.

The solvent dependence of the emission maximum of **I** is qualitatively similar to that of 4-AP. In aprotic solvents, the emission maximum of both exhibits a relatively small red shift with an increase in polarity. In going from dioxane to acetonitrile, the emission maximum of 4-AP exhibits a red shift of 23 nm (from 435 to 458 nm),[19d] whereas **I** displays a red shift of only 5 nm (from 390 to 395 nm). However, in protic solvents such as alcohol and water, there is a very dramatic red shift of the emission maximum for both of them. Compared to the emission maximum in dioxane, in water, the emission maximum of 4-AP (550 nm) is red-shifted by 115 nm,[19d] whereas **I** exhibits a 70 nm red shift to 460 nm.

There is a drastic difference in the solvent dependence of the emission quantum yield (ϕ_f) and lifetime (τ_f) of **I** from those in the case of 4-AP. ϕ_f of 4-AP in dioxane (0.7) is 70 times higher than that in water (0.01), whereas τ_f in dioxane (15 ns) is 15 times longer than that in water (1.1 ns).[19d] But ϕ_f of **I** in dioxane (0.006) is 65 times lower than that in water (0.4), whereas τ_f in dioxane (0.2 ns) is 40 times shorter than that in water (8 ns).

Several groups have investigated the nonradiative pathways of 4-AP and its derivatives.[19,20] However, the exact cause of the dramatic reduction of ϕ_f and τ_f of 4-AP in protic solvents is not yet understood fully. The reduction of ϕ_f and τ_f of 4-AP in protic solvents indicates a marked increase in the nonradiative decay rate. This may be due to either a nonradiative pathway involving an interaction with the protic solvents or a change in the energy gap between the various excited states ($n\pi^*$ and $\pi\pi^*$ excited states).

Harzu et al.[19a] earlier proposed that in a protic solvent the main nonradiative pathway of 4-AP is solvent-mediated proton transfer from the imino group to the oxygen atom of the carbonyl group. However, the emission properties of the imino *N*-alkyl derivative of 4-AP are found to be very similar to those of 4-AP.[19c] This rules out the possibility that transfer of the imino proton is the main nonradiative pathway of 4-AP.

One may argue that in 4-AP the nonradiative process involves transfer of the amino protons to the carbonyl oxygen. If this were true, bromoacetylation of the amino group (as in **I**) would largely inhibit proton transfer and hence the nonradiative decay. As a result, both in water and in dioxane, **I** would exhibit similar emission properties, and in both solvents, it should display a very high emission quantum yield and a long lifetime. The marked differences of the emission properties of **I** in these two solvents indicate that the solvent dependence of the photophysical properties of **I** (and 4-AP) is not due to the transfer of the amino proton.

The increase in the emission quantum yield of **I** in a protic solvent compared to that in an aprotic solvent is similar to the fluorescence enhancement of many heterocycles on complexation with water in a supersonic jet.[20,21] In a supersonic jet, the emission lifetime of a heterocyle (acridone[21] and even 4-AP[20]) in a cluster involving a protic solvent (water and methanol) is found to be longer than that of the free molecule. To explain this, Mitsui and Ohsmima[21] proposed that the hydrogen-bond interaction of **I** with water or methanol increases the energy gap between the $n\pi^*$ and $\pi\pi^*$ excited states, and this causes a decrease in the nonradiative decay rate. Following this, we ascribe the increase in ϕ_f and τ_f of **I** in a protic solvent to the marked decrease in the nonradiative decay rate arising from the increase in the energy gap between the $n\pi^*$ and $\pi\pi^*$ excited states. However, it may be pointed out that even 4-AP and its methyl derivative display an increase in lifetime on complexation with water and methanol molecules in a supersonic jet.[20] This is in sharp contrast to the decrease in the emission lifetime of 4-AP in liquid solutions in water and methanol.

The slow solvation dynamics of water in microemulsions in the case of **I** is very similar to that exhibited by many probes[1,13] including 4-AP.[13a] Several recent simulations[22] have indicated such slow solvation in a microemulsion,[22a] micelle,[22b] and liquid−liquid interfaces.[22c] This indicates that **I** is a good solvation probe for studying solvation in organized assemblies. Having established this, we finally consider the solvation dynamics at a selected location of a protein, GlnRS.

The solvation time of **I** covalently attached to GlnRS exhibits two components of 40 and 580 ps. It may be noted that the 40-ps component is similar to the 38-ps component reported by Zewail et al.[7] for tryptophan of the protein SC, whereas the 580-ps component is similar to the 530-ps component reported by Fleming et al. for eosin noncovalently bound to lysozyme.[3] We did not observe any long component on the 1000 ps time scale as observed for DCM in HSA.[4] This indicates that in this case the covalently attached probe is not located deep inside the protein. This is understandable because, as discussed earlier, the −SH group of cysteine 206 of GlnRS is quite exposed.

Using the RASMOL program,[23] we have estimated the distance of the sulfur atoms from the protein surface for cystein 206 as well as for the less-reactive cysteines,[16] 330, 525, 229, and 61. Interestingly, in all cases, the sulfur atom is situated at a depth of 5−8 Å from the surface. The structure of the protein GlnRS around residue 206 is shown in Figure 9. Even though residue 206 is close to the surface, the sulfur atom is at a depth of approximately 7.5 Å from the surface and is embedded in a cleft. A simple MM2 calculation indicates that the distance between the S atom of the protein and the amino nitrogen of the probe is about 3 Å. If we subtract the distance of about 3 Å from the sulfur to the amino nitrogen of **I**, the nitrogen atom is situated at a depth of 4.5 Å from the surface for residue 206 and at 2−5 Å for other cysteines. Obviously, whereas one end of the probe (around the amino nitrogen) remains buried inside the protein surface, the other part sticks partially out of the protein. The motion of the water molecules trapped in the cleft around the probe just below the protein surface is likely to be highly restricted. This appears to be the origin of the slow components (40 and 580 ps) of solvation dynamics.

Apart from the confined water molecules, other polar entities (e.g., the polar side chains of a protein or the peptide linkage) may also contribute to the solvation dynamics. The components

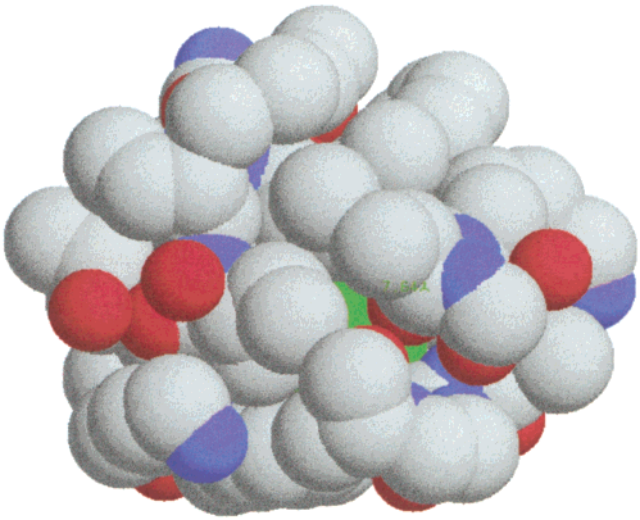

Figure 9. Space-filling model of the area of the protein GlnRS around residue 206 (green). The rest of the model is colored according to the CPK scheme.

of solvation dynamics (40 and 580 ps) detected in the present work cannot be ascribed to the chain dynamics of macromolecules that occurs on a much slower time scale of 100 ns.[24] Formamide resembles the peptide linkage. In bulk formamide and *N*,*N*-dimethyl formamide, the solvation dynamics occurs on a $\leq$1 ps time scale, which is much faster than the observed components (40 and 580 ps). Though one cannot rule out the contribution of restricted movement of the polar segments of the protein, the major source of the slow solvation dynamics is the constrained water molecules.

Nandi and Bagchi[2] earlier proposed that in aqueous protein solutions there are two kinds of water molecules. The "bound" water molecules attached to the protein are slow because their motion becomes coupled with that of the protein. The free water molecules are those in the bulk, and there is a dynamic equilibrium between the bound and free water. Because all the water molecules in the immediate vicinity of the protein are essentially "bound", they display slow solvation dynamics. In the present case, both of the components (40 and 580 ps) of the bimodal decay are much slower than that in bulk water ($\sim$1 ps). The bimodality may arise because the different parts of the probe are exposed to water molecules of different dynamical properties.

It may be recalled that according to the MD simulation by Rocchi et al.[25] the dynamics of the water molecules at a short distance ($<$4 Å) from the surface of a protein plastocyanin is significantly slow compared to that of bulk water. However, at a large distance ($>$14 Å) from the surface, the dynamics becomes very fast and bulklike.[25] In the present case, the major part of the dynamics is due to the water molecules buried just below the surface, and hence the observed slow dynamics is consistent with the MD simulations carried out by Rocchi et al.[25]

Though the probe is most likely to be attached to the most reactive cysteine, 206, one cannot rule out the possibility that other cysteins may also get labeled, at least partially. However, one should note that the other sulfhydryls are also at a depth from the protein surface that is similar to that for 206. Thus, in the present study, we have detected the dynamics of water just below the protein surface. In summary, the slower solvation dynamics detected in this work reflects the restricted motion of the water molecules occupying the constricted space of a cleft, slightly below the surface at a depth of 2$-$5 Å.

5. Conclusions

In this work, we have used the bromoacetyl derivative of 4-AP (**I**) as a new solvation probe for studying solvation dynamics in an organized medium, namely, microemulsion, and we then studied the solvation dynamics at a well defined site within a protein by covalently attaching the probe **(I)** to a protein GlnRS. The photophysics of **I** is fundamentally different from that in the parent compound, and we ascribe the marked decrease in the nonradiative rates of **I** in polar and protic solvents (water or alcohol) to the increase in the energy gap between the nπ* and $\pi\pi$* states as a result of hydrogen bonding. The solvation dynamics of **I** in a microemulsion is similar to that of other probes and reveals very slow relaxation with an average solvation time of 800 $\pm$ 50 ps. In GlnRS, a part of the probe remains buried at a depth of 5$-$8 Å from the surface of the protein. At this location, the solvation dynamics of water molecules exhibit a major component of 40 ps and a minor component of 580 ps. This indicates at that this site, where major part of the probe is buried just inside the protein surface, the water molecules are highly constrained and display very slow solvation dynamics.

Acknowledgment. Thanks are due to the Council of Scientific and Industrial Research (CSIR) and the Department of Science and Technology (DST) for generous research grants. D.M., S.S., and D.S. thank CSIR for research fellowships.

References and Notes

(1) (a) Nandi, N.; Bhattacharyya, K.; Bagchi, B. *Chem. Rev.* **2000**, *100*, 2013. (b) Bhattacharyya, K.; Bagchi, B. *J. Phys. Chem. A* **2000**, *105*, 10609. (c) Levinger, N. E. *Curr. Opin. Colloid Interface Sci.* **2000** *5*, 118. (d) Halle, B. In *Hydration Processes in Biology: Theoretical and Experimental Approaches*; Bellissent-Funnel, M.-C., Ed.; IOS Press: Amsterdam, 1999; pp 233$-$249.

(2) (a) Nandi, N.; Bagchi, B. *J. Phys. Chem. B* **1997**, *101*, 10954. (b) Nandi, N.; Bagchi, B. *J. Phys. Chem. A* **1998**, *102*, 8217.

(3) Jordandies, X. J.; Lang, M. J.; Song, X.; Fleming, G. R. *J. Phys. Chem. B* **1999**, *103*, 7995.

(4) Pal, S. K.; Mandal, D.; Sukul, D.; Sen, S.; Bhattacharyya, K. *J. Phys. Chem. B* **2001**, *105*, 1438.

(5) (a) Pierce, D. W.; Boxer, S. G. *J. Phys. Chem.* **1992**, *96*, 5560. (b) Bashkin, J. S.; McLendon, G.; Mukamel, S.; Marohn, J. *J. Phys. Chem.* **1990**, *94*, 4757.

(6) Zhong, D.; Pal, S. K.; Zewail, A. H. *ChemPhysChem* **2001**, *2*, 219.

(7) Pal, S. K.; Peon, J.; Zewail, A. H. *Proc. Natl. Acad. Sci. U.S.A.* **2002**, *99*, 1763.

(8) Toptygin, D.; Savtchenko, R. S.; Medow, N. D.; Brand, L. *J. Phys. Chem. B* **2001**, *105*, 2043.

(9) (a) Vajda, S.; Jimenez, R.; Rosenthal, S. J.; Fidler, V.; Fleming, G. R.; Castner, E. W., Jr. *J. Chem. Soc., Faraday Trans.* **1995**, *91*, 867. (b) Nandi, N.; Bagchi, B. *J. Phys. Chem.* **1996**, *100*, 13914. (c) Sen, S.; Sukul, D.; Dutta, P.; Bhattacharyya, K. *J. Phys. Chem. A* **2001**, *105*, 10635.

(10) (a) Brauns, E. B.; Madaras, M. L.; Coleman, R. S.; Murphy, C. J.; Berg, M. A. *Phys. Rev. Lett.* **2002**, *88*, 158101-1. (b) Brauns, E. B.; Madaras, M. L.; Coleman, R. S.; Murphy, C. J.; Berg, M. A. *J. Am. Chem. Soc.* **1999**, *121*, 11644.

(11) Pal, S. K.; Sukul, D.; Mandal, D.; Bhattacharyya, K. *J. Phys. Chem. B* **2000**, *104*, 4529.

(12) Sen, S.; Sukul, D.; Dutta, P.; Bhattacharyya, K. *J. Phys. Chem. B* **2002**, *106*, 3763.

(13) (a) Das, S.; Datta, A.; Bhattacharyya, K. *J. Phys. Chem. A* **1997**, *101*, 3299. (b) Willard, D. M.; Levinger, N. E. *J. Phys. Chem. B* **2000**, *104*, 11075. (c) Lundgren, J. S.; Heitz, M. P.; Bright, F. V. *Anal. Chem.* **1995**, *67*, 3775. (d) Riter, R. E.; Undiks, E. P.; Kimmel, J. R.; Pant, D. D.; Levinger, N. E. *J. Phys. Chem. B* **1998**, *102*, 7931. (e) Shirota, H.; Horie, K. *J. Phys. Chem. B* **1999**, *103*, 1437.

(14) (a) Pal, S. K.; Sukul, D.; Mandal, D.; Sen, S.; Bhattacharyya, K. *Chem. Phys. Lett.* **2000**, *327*, 91. (b) Hara, K.; Kuwabara, H.; Kajimoto, O. *J. Phys. Chem. A* **2001**, *105*, 7174.

(15) (a) Lakowciz, J. R. *Principles of Fluorescence Spectroscopy*, 2nd ed.; Kluwer: 1999. (b) Miller, D. P. *Curr. Opin. Struct. Biol.* **1996**, *6*, 637. (c) Robinson, B. H.; Mailer, C.; Drobney, G. *Annu. Rev. Biophys. Biomol. Struct.* **1997**, *26*, 629. (d) Quitevis, E. L.; Marcus, A. H.; Fayer, M. D. *J.*

Phys. Chem. **1993**, *97*, 5762. (e) Sen, S.; Sukul, D.; Dutta, P.; Bhattacharyya, K. *J. Phys. Chem. A* **2001**, *105*, 7495.

(16) Rould, M. A.; Perona, J. J.; Soll, D.; Steitz, T. A. *Science (Washington, D.C.)* **1989**, *246*, 1135.

(17) (a) Bhattacharyya, T.; Roy, S. *Biochemistry* **1993**, *32*, 9268. (b) Bhattacharyya, T.; Bhattacharyya, A.; Roy, S. *Eur. J. Biochem.* **1991**, *200*, 739.

(18) Maroncelli, M.; Fleming, G. R. *J. Chem. Phys.* **1987**, *86*, 6221.

(19) (a) Harzu, T. O.; Huizer, A. H.; Varma, C. A. G. O. *Chem. Phys.* **1995**, *200*, 215. (b) Saroja, G.; Ramachandram, B.; Saha, S.; Samanta, A. *J. Phys. Chem. B* **1999**, *103*, 2906. (c) Saroja, G.; Samanta, A. *J. Chem. Soc., Faraday Trans.* **1996**, *92*, 2697. (d) Soujanya, T.; Krishna, T. S. R.; Samanta, A. *J. Phys. Chem.* **1992**, *96*, 8544.

(20) Andrews, P. M.; Beyer, M. B.; Troxler, T.; Topp, M. R. *Chem. Phys. Lett.* **1997**, *271*, 19.

(21) Mitsui, M.; Ohshima, Y. *J. Phys. Chem. A* **2000**, *104*, 8638.

(22) (a) Senapati, S.; Chandra, A. *J. Phys. Chem. B* **2001**, *105*, 5106. (b) Balasubramanian, S.; Bagchi, B. *J. Phys. Chem. B* **2001**, *105*, 12529. (c) Michael, D.; Benjamin, I. *J. Chem. Phys.* **2001**, *114*, 2817. (d) Faeder, J.; Ladayani, B. M. *J. Phys. Chem. B* **2001**, *105*, 11148.

(23) *RASMOL: UCB enhanced*, version 2.5; http://mc2.cchem.berkeley.edu/Rasmol/.

(24) (a) Cassol, R.; Ge, M.-T.; Freed, J. H. *J. Phys. Chem. B* **1997**, *101*, 8782. (b) Sung-Suh, M. M.; Kevan, L. *J. Phys. Chem. A* **1997**, *101*, 1414.

(25) Rocchi, C.; Bizzarri, A. R.; Cannistaro, S. *Phys. Rev. E: Stat. Phys., Plasmas, Fluids, Relat. Interdiscip. Top.* **1998**, *57*, 3315.